Nanoscale

Cite this: *Nanoscale*, 2012, **4**, 5852

www.rsc.org/nanoscale

COMMUNICATION

Enhanced light emission of GaN-based diodes with a NiO_x/graphene hybrid electrode

Yiyun Zhang,[a] Xiao Li,[b] Liancheng Wang,[a] Xiaoyan Yi,[a] Dehai Wu,[b] Hongwei Zhu*[bc] and Guohong Wang[a]

Received 5th May 2012, Accepted 6th August 2012
DOI: 10.1039/c2nr31986a

A NiO_x buffer layer is introduced in GaN-based light-emitting diodes to form low resistance ohmic contacts between p-type GaN and graphene conductive electrodes, leading to improved performance with lower operating voltage and higher light output power.

GaN-based light emitting diodes (LEDs) have attracted extensive attention in the past few decades due to their great advantages of high brightness, low energy consumption, and long lifetime. They have been widely used in various applications including general lighting, traffic lights, automobile headlights, and backlight units for liquid crystal displays.[1] Recently, use of graphene as transparent conducting electrodes in GaN-based LEDs has been extensively investigated because of its excellent optical and electrical properties.[2–5] Graphene is considered as an ideal candidate to replace conventional indium tin oxide (ITO) electrodes. However, as a result of low hole concentration and high work function of p-GaN, it is hard for the current spreading layer to form a good ohmic contact with p-GaN.[6] In addition, the work function mismatch of graphene (~4.8 eV) and p-GaN (~7.5 eV) will lead to a high contact barrier that hinders the movement of electrons and increases the operating voltage of LEDs with graphene electrodes. Therefore, forming a good ohmic contact with the p-GaN layer is a key point to improve the performance of GaN-based LEDs with graphene transparent electrodes. To solve this problem, previous studies have developed several effective approaches by inserting ITO quantum dots[7,8] and metal sheets[9] between graphene and the p-GaN layer or by modifying the work function of graphene[10] to decrease the contact resistance. With these methods, the performance, especially the electrical properties of LEDs with graphene transparent electrodes, has been greatly improved. However, the operating voltage of ~4.0 V (at 20 mA) reported previously for the LEDs with graphene electrodes still needs to be further decreased, when considering "state-of-the-art" LEDs using other transparent electrodes like ITO and ZnO transparent electrodes the operating voltage is 3.2–3.4 V (at 20 mA).[11,12]

In this work, a very thin NiO_x buffer layer (1–2 nm) is introduced below the graphene film to improve its ohmic contact with the underlying p-GaN layer. With a transparency as high as ~90% to the visible light, the NiO_x/graphene hybrid film serves as a good electrode for GaN-based LEDs. The large work function of the NiO_x interlayer reduces the contact barrier at the graphene/p-GaN layer interface. Moreover, the high p-type carrier concentration of NiO_x caused by the nickel vacancies and/or oxygen interstitials makes it easier for graphene to form ohmic contacts with the p-GaN layer[13–25] and consequently improves the LED performance.

Fig. 1(a) shows the schematic structure of the LED device with NiO_x/graphene conducting electrodes. The LED multilayers were first grown on 2-inch *c*-plane (0001) sapphire substrates *via* metal–organic chemical vapor deposition (CVD). The GaN epitaxial structure consists of a 50 nm thick low-temperature-grown GaN buffer layer, a 2 μm thick undoped GaN layer, a 2 μm thick heavily Si-doped n-type GaN layer, 5 pairs of InGaN (3 nm)/GaN (12 nm) multiple quantum wells (MQWs) and a 100 nm thick Mg-doped p-type GaN layer. After deposition of a 2 nm thick Ni film on the p-type GaN layer by an electron beam system, the GaN wafers were annealed at 400 °C in air for 3 min. Then graphene films were transferred onto the GaN wafers. Conventional mesa structure LEDs ($225 \times 175\ \mu m^2$) were fabricated after an inductively coupled plasma etching process and p–n metal electrode deposition. Graphene films

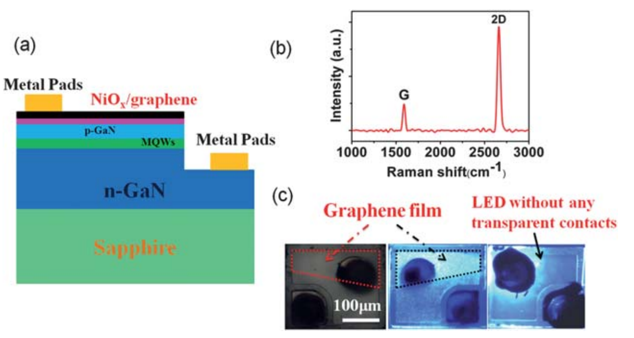

Fig. 1 (a) Schematic structure of the LED device with the NiO_x/graphene electrode. (b) Raman spectrum of the graphene film. (c) Photographs of LED chips with the NiO_x/graphene electrode and without any transparent electrode.

[a]*Semiconductor Lighting Technology Research and Development Center, Institute of Semiconductors, Chinese Academy of Sciences, Beijing 100083, China*
[b]*Department of Mechanical Engineering, Key Laboratory for Advanced Manufacturing by Materials Processing Technology, Tsinghua University, Beijing 100084, China. E-mail: hongweizhu@tsinghua.edu.cn; Fax: +86 10 62773637; Tel: +86 10 62781065*
[c]*Center for Nano and Micro Mechanics (CNMM), Tsinghua University, Beijing 100084, China*

used here were prepared on copper foils by CVD. In detail, the copper foils were heated to 1000 °C under Ar (500 mL min^{-1}) and H_2 (50 mL min^{-1}). After reaching 1000 °C, Ar was turned down to 200 mL min^{-1} and H_2 to 20 mL min^{-1}. A small amount of CH_4 (5–10 mL min^{-1}) was then introduced into the reaction tube at ambient pressure. After 10 min of reaction-gas mixture flow, the samples were rapidly cooled to room temperature. Then the copper foils were removed in $FeCl_3$ aqueous solution and graphene films were released floating on the liquid surface. After that, graphene films were transferred into deionized water to remove the residual impurities. Fig. 1(b) shows a typical Raman spectrum of the graphene film. The presence of dominant G band (~1590 cm^{-1}) and 2D band (~2658 cm^{-1}) reveals the high quality of graphene. Fig. 1(c) shows the optical photographs of a LED chip with the graphene/NiO_x hybrid electrode before and after applying 1 mA current. One can see a clear light output power enhancement in the area of the LED with the NiO_x/graphene hybrid electrode. In addition, comparing with LEDs without any transparent contact, the uniformity of light emission below the NiO_x/graphene hybrid electrode is greatly improved. It is worthy to note that, to illustrate the important role as the conducting film that graphene plays in the NiO_x/graphene hybrid electrode, a LED chip partly covered with graphene film is selected, as shown in the middle panel of Fig. 1(c).

To investigate the impact of the thin NiO_x buffer layer on the light extraction efficiency of the LED devices, the visible transmittance of the NiO_x/graphene hybrid structure was first examined. Fig. 2(a) shows the transmission spectra of different conducting electrodes used in our experiment. The NiO_x (~1 nm)/graphene layer exhibits a transparency of nearly 90% to visible light. In addition, it is worth noting that the transparency of NiO_x(~1 nm)/graphene to blue and ultraviolet light is much higher than that of a 280 nm ITO layer, suggesting its application potential in transparent conducting electrodes for blue or ultraviolet LEDs. To further reveal the role of graphene in the NiO_x/graphene hybrid electrodes, we tested the sheet resistances of the NiO_x buffer layer (1–2 nm), NiO_x/graphene, graphene, NiO_x/ITO, and 280 nm ITO layer. As shown in Fig. 2(b), the sheet resistance of NiO_x buffer layers (>10 kΩ) is much higher than that of graphene (~kΩ) and ITO (~20 Ω). The sheet resistance of NiO_x/graphene and NiO_x/ITO hybrid electrodes is almost the same as that of bare graphene and ITO, respectively, suggesting that the conducting performance of the NiO_x/graphene hybrid is determined by the conductivity of graphene. The underlying NiO_x buffer layer in the hybrid electrodes mainly serves as a contact layer to the underneath p-GaN layer.

To characterize the NiO_x/graphene contact with the underlying p-type GaN layer, the current–voltage (*I–V*) curves of different LED devices were collected, as illustrated in Fig. 3(a). By inserting a thin NiO_x buffer layer, the *I–V* curve becomes more linear compared with the samples without the NiO_x layer, which indicates that the ohmic contact between graphene and the p-GaN layer is greatly improved. Meanwhile, a steeper slope of the *I–V* curve than that of the ITO layer is observed, revealing a lower contact resistance than ITO/p-GaN obtained by introducing the NiO_x layer. The specific contact resistance was further characterized using a circular transmission line model (CTLM). The CTLM pattern is presented in the inset of Fig. 3(a). The CTLM results show that the contact resistance between the NiO_x/graphene and p-GaN is 5.9×10^{-4} Ω cm^2, which is about 2–3 orders lower than that of the graphene/p-GaN structure (10^{-1} to 10^{-2} Ω cm^2). And it is also much lower than that of the ITO/p-GaN or ITO/NiO_x/p-GaN structure (~10^{-3} Ω cm^2). The $R_t - \ln(R/r)$ curves of different transparent electrodes are shown in Fig. 3(b), where R_t represents the resistance of the transparent contact.

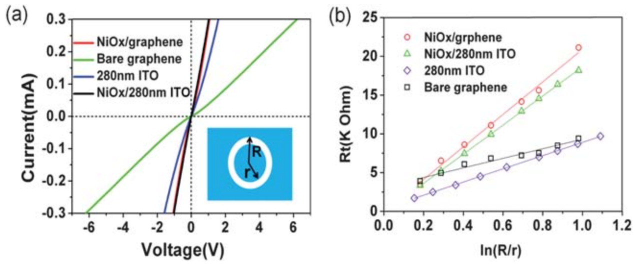

Fig. 3 (a) Current–voltage (*I–V*) curves. (b) $R_t - \ln(R/r)$ curves of different transparent contacts.

Fig. 4(a) shows the *I–V* curves of the LED devices with different transparent electrodes. At an injection current of 20 mA, the voltage of the LED device with the NiO_x/graphene hybrid electrode is dramatically reduced from 6.15 V to 3.65 V. Such a large drop in the voltage is due to the fact that the ohmic contact between graphene and p-GaN has been greatly improved by inserting the NiO_x buffer layer. The voltage of the LED with the NiO_x/graphene hybrid electrode at an injection current of 20 mA is a little higher than that of the LED with the 280 nm ITO (~3.2 V), which can be explained by the fact that the series resistance of the graphene film is still larger than that of the 280 nm ITO layer. Based on the fact that the operating voltage of LED devices is greatly related to the series resistance of the transparent conducting electrodes, one may predict that the voltage of the LEDs would be further decreased if the quality of the graphene films from CVD was improved.[8,10]

The light output power (LOP) curves of the LED devices with different transparent conducting electrodes are shown in Fig. 4(b).

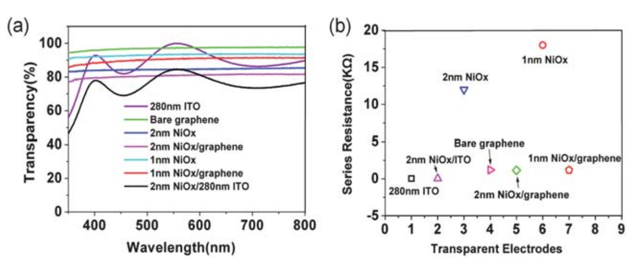

Fig. 2 (a) Transmission spectra. (b) Sheet resistances of NiO_x (1, 2 nm), NiO_x/graphene, graphene, NiO_x/ITO, and 280 nm ITO.

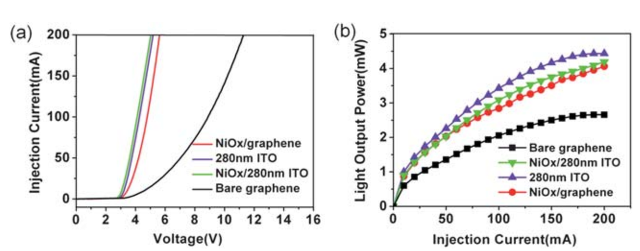

Fig. 4 (a) Current–voltage (*I–V*) curves. (b) LOP–*I* curves of LED devices with different transparent conducting electrodes.

The LOP of the LED with NiO_x/graphene is much higher than those of LEDs without NiO_x. At an injection current of 20 mA, the LOP of the LED device with the NiO_x/graphene hybrid electrode can be improved by 57% compared with the LED with a bare graphene electrode. This enhancement is also attributed to the improved ohmic contact between graphene and p-GaN. The LED efficiency will dramatically decrease if the injection current is blocked due to the weaker current spreading ability of transparent conducting electrodes.[26–28] Considering the fact that the quality of the CVD-grown graphene film can be improved and the series resistance will be further decreased, although the LOP of the LED devices with NiO_x/graphene electrodes is still lower than that of the LED with the ITO electrode, the proposed approach provides a rational yet effective way to improve the LED performance.

Fig. 5(a) shows the X-ray photoelectron spectroscopy (XPS) spectra of $Ni2p_{3/2}$ before and after the deposited Ni layer was annealed in air at 400 °C. Significant difference can be observed in the binding energy of $Ni2p_{3/2}$ for the annealed Ni film. A Ni^{2+} peak (854.5 eV) and two Ni^{3+} peaks (861.3 eV, 855.7 eV) are clearly identified, suggesting the formation of NiO and Ni_2O_3, respectively. In the O1s spectra shown in Fig. 3(b), two distinct peaks (529.5 eV, 531.5 eV) can be detected, which correspond to the binding states of Ni^{3+} and Ni^{2+}.[25] Holes will be bound by the nearby Ni^{2+} vacancies in the annealed NiO film, which produce Ni^{3+} ions. These bound holes will accept electrons and turn NiO into a p-type semiconductor. The hole concentration of the NiO film can reach a level of 1.3×10^{19} cm^{-3}, which greatly improves the ohmic contact with the p-GaN layer.[13,14]

The equilibrium energy band diagrams of graphene/p-GaN and graphene/NiO_x/p-GaN heterostructures are shown in Fig. 5(c). E_v, E_c and E_f represent the top of the valence band, the bottom of the conduction band and the Fermi level, respectively. In the graphene/p-GaN heterostructure, the height and width of the contact barrier between graphene and p-GaN are defined as φ_B and ΔD. In the NiO_x/p-GaN heterostructure, the widths of the contact barrier in the NiO_x and p-GaN are defined as Δd_{NiOx} and $\Delta d_{p\text{-}GaN}$ correspondingly. Compared with the contact barrier between graphene and p-GaN, the energy band bending at the NiO_x/p-GaN interface ($\Phi_{p\text{-}GaN}$, $\Psi_{NiOx} < \varphi_B$) is much smaller due to the large work function of NiO_x. In addition, the ultrathin p-type NiO_x layer reduces the contact barrier width at the NiO_x/p-GaN interface (Δd_{NiOx}, $\Delta d_{p\text{-}GaN} < \Delta D_{p\text{-}GaN}$). Therefore, by introducing the NiO_x buffer layer, electrons can pass through the barrier more easily.[21]

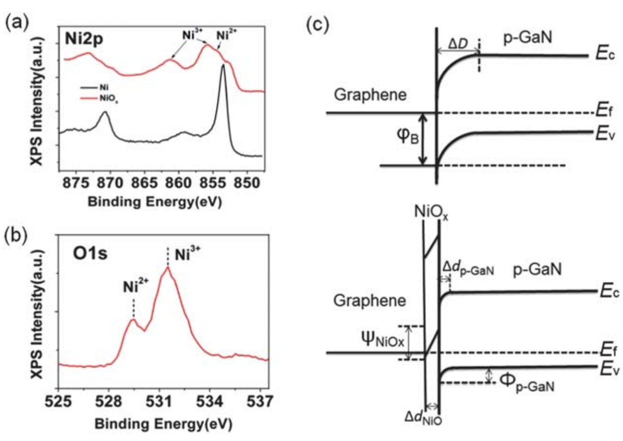

Fig. 5 XPS spectra of the annealed Ni layer: (a) $Ni2p_{3/2}$ and (b) O1s. (c) Energy band diagrams of graphene/p-GaN and graphene/NiO_x/p-GaN heterostructures.

Conclusions

In summary, GaN-based blue LEDs with NiO_x/graphene hybrid electrodes were fabricated and their optoelectronic properties were investigated. By inserting an extra thin NiO_x buffer layer, a low contact resistance of 5.9×10^{-4} Ω cm^2 was obtained between graphene and the p-GaN layer, resulting in a dramatic decrease in the forward voltage of LED with graphene electrodes. The large work function of NiO_x reduced the contact barrier between graphene and the p-GaN layer and the high p-type carrier concentration of NiO_x also facilitated the formation of good ohmic contacts with the p-GaN layer. Meanwhile, the light output power of LED with NiO_x/graphene hybrid electrodes was greatly improved. The proposed method provides an effective way to improve the performance of the GaN-based LEDs with graphene electrodes.

This work was supported by the National High Technology Program of China (2011AA03A105 and 2011AA03A103), National Natural Science Foundation of China (60806001 and 50972067), and National Basic Research Program of China (2011CB301904 and 2011CB013000).

Notes and references

1 E. F. Schubert and J. K. Kim, *Science*, 2005, **308**, 1274.
2 K. Chung, C.-H. Lee and G.-C. Yi, *Science*, 2010, **330**, 655.
3 B.-J. Kim, M. A. Mastro, J. Hite, C. R. Eddy, Jr and J. Kim, *Opt. Express*, 2010, **18**, 23030.
4 G. Jo, M. Choe, C.-Y. Cho, J. H. Kim, W. Park, S. Lee, W.-K. Hong, T.-W. Kim, S.-J. Park, B. H. Hong, Y. H. Kahng and T. Lee, *Nanotechnology*, 2010, **21**, 175201.
5 Y. Zhang, L. Wang, X. Li, X. Yi, N. Zhang, J. Li, H. Zhu and G. Wang, *J. Appl. Phys.*, 2012, **111**, 114501.
6 J. O. Song, J.-S. Ha and T.-Y. Seong, *IEEE Trans. Electron Devices*, 2010, **57**, 42.
7 T. H. Seo, K. J. Lee, T. S. Oh, Y. S. Lee, H. Jeong, A. H. Park, H. Kim, Y. R. Choi, E.-K. Suh, T. V. Cuong, V. H. Pham, J. S. Chung and E. J. Kim, *Appl. Phys. Lett.*, 2011, **98**, 251114.
8 T. H. Seo, K. J. Lee, A. H. Park, C.-H. Hong, E.-K. Suh, S. J. Chae, Y. H. Lee, T. V. Cuong, V. H. Pham, J. S. Chung, E. J. Kim and S.-R. Jeon, *Opt. Express*, 2011, **19**, 23111.
9 J. M. Lee, H. Y. Jeong, K. J. Choi and W. Park, *Appl. Phys. Lett.*, 2011, **99**, 041115.
10 S. Chandramohan, J. H. Kang, Y. S. Katharria, N. Han, Y. S. Beak, K. B. Ko, J. B. Park, H. K. Kim, E.-K. Suh and C.-H. Hong, *Appl. Phys. Lett.*, 2012, **100**, 023502.
11 S.-M. Pan, R.-C. Tu, Y.-M. Fan, R.-C. Yeh and J.-T. Hsu, *IEEE Photonics Technol. Lett.*, 2003, **15**, 646.
12 J.-H. Lim, D.-K. Hwang, M.-K. Kwon, I.-K. Park, S.-I. Na and S.-J. Park, *Phys. Status Solidi C*, 2005, **2**, 2533.
13 H. Sato, T. Minami, S. Takata and T. Yamada, *Thin Solid Films*, 1993, **236**, 27.
14 J.-K. Ho, C.-S. Jong, C. C. Chiu, C.-N. Huang, C.-Y. Chen and K.-K. Shih, *Appl. Phys. Lett.*, 1999, **74**, 1275.
15 S.-H. Kang, D.-K. Hwang and S.-J. Park, *Appl. Phys. Lett.*, 2005, **86**, 211902.
16 J. O. Song, K.-K. Kim, S.-J. Park and T.-Y. Seong, *Appl. Phys. Lett.*, 2003, **83**, 479.
17 J. Narayan, H. Wang, T.-H. Oh, H. K. Choi and J. C. C. Fan, *Appl. Phys. Lett.*, 2002, **81**, 3978.
18 D. Mistele, F. Fedler, H. Klausing, T. Rotter, J. Stemmer, O. K. Semchinova and J. Aderhold, *J. Cryst. Growth*, 2001, **230**, 564.
19 C.-T. Lee, Y.-J. Lin and T.-H. Lee, *J. Electron. Mater.*, 2003, **32**, 341.

20 T. Maeda, Y. Koide and M. Murakami, *Appl. Phys. Lett.*, 1999, **75**, 4145.
21 C.-S. Lee, Y.-J. Lin and C.-T. Lee, *Appl. Phys. Lett.*, 2001, **79**, 3815.
22 Y.-J. Lin, Z.-D. Li, C.-W. Hsu, F.-T. Chien, C.-T. Lee, S.-T. Shao and H.-C. Chang, *Appl. Phys. Lett.*, 2003, **82**, 2817.
23 J.-K. Ho, C.-S. Jong, C. C. Chiu, C.-N. Huang, K.-K. Shih, L.-C. Chen, F.-R. Chen and J.-J. Kai, *J. Appl. Phys.*, 1999, **86**, 4491.
24 Z. Z. Chen, Z. X. Qin, Y. Z. Tong, X. D. Hu, T. J. Yu, Z. J. Yang, L. S. Yu, G. Y. Zhang, W. L. Zheng, Q. J. Jia and X. M. Jiang, *J. Appl. Phys.*, 2004, **96**, 2091.
25 K. S. Kim and N. Winograd, *Surf. Sci.*, 1974, **43**, 625.
26 Y.-J. Liu, C.-C. Huang, T.-Y. Chen, C.-S. Hsu, T.-Y. Tsai and W.-C. Liu, *IEEE Photonics Technol. Lett.*, 2011, **23**, 1037.
27 T. Tian, Y. Zhang, X. Yi, Z. Liu, J. Li and G. Wang, *Electrochem. Solid-State Lett.*, 2012, **1**, R5.
28 H.-Y. Ryu and J.-I. Shim, *Opt. Express*, 2011, **19**, 2886.